

FORCE DISTRIBUTION BETWEEN THE
CORE AND SUBGRADE STRUCTURE OF HIGH RISE BUILDINGS
SUBJECTED TO LATERAL LOAD INDUCED FORCES

by

G.L. Bevan-Pritchard, P.Eng.

and

E. Man, M.A.Sc., P.Eng.
McKenzie Snowball Skalbania & Associates Ltd.

and

D.L. Anderson
Department of Civil Engineering, U.B.C.

ABSTRACT

This paper discusses the distribution of the lateral load induced moments and shears between the building core and the subgrade structure, in the region of the subgrade structure, of typical high rise buildings. The influence of the bending and shear stiffness of the core, of the foundation or subgrade structure walls, and of the floors of the subgrade structure has been investigated for the core base assumed either fully fixed or pinned. It is seen that the core moments and shears depend most on the degree of base fixity, and that the in-plane stiffness of the floors of the subgrade structure also has considerable influence.

The in-plane stiffness of the floors has been determined using a finite element analysis, and a semi-empirical formula derived by which the stiffness can be estimated for structures with a single centrally located core.

INTRODUCTION

Modern multi-storey buildings are commonly constructed with a service core (typically containing stair shafts, elevator shafts and lobbies) projecting up from the foundation through several levels of underground parking, Figure 1. It is common practice to design this service core to provide lateral resistance to earthquake and wind forces acting on the superstructure. The moment and shear forces are carried by the core down to the top of the subgrade structure or parking levels. At this point the subgrade structure starts to pick up some of the lateral load, and it is the intent of this paper to examine the effect of the core stiffness, relative to the stiffness of the subgrade structure, on how the moments and shears are transmitted to the foundation.

A model was designed to reflect the below grade structure of the buildings, and the geometric properties such as moments of inertia and areas, as well as the degree of fixity of the service core base, were then varied to cover a range of practical buildings. Numerous computer runs were made to determine the effect of these variables on the distribution of the moments and shears between the below grade service core and the rest of the subgrade structure.

MODELLING OF THE SUBGRADE STRUCTURE

The underground portion of the structure was modelled as shown in Figure 2. The service core is modelled as a line element having both bending and shear stiffness. The perimeter foundation wall is also modelled as a line element with bending and shear stiffness. Springs that model the in plane bending, shear and axial stiffness of the parking slabs connect the service core element to the foundation wall element.

The determination of the spring constant and the derivation of a formula for estimating this constant is discussed in the second half of the paper.

For modelling purposes a moment of 100 K-FT and a shear of 1K was applied to the service core just above the ground level. This ratio of shear to moment is compatible with the ratio of shear to moment one would expect to obtain in the analysis of a 20 storey building subjected to earthquake generated loads. In this study the shear and moment will be applied separately to emphasize the individual contributions of the two forces to the shears and moments developed in the service core below ground.

ANALYSIS AND OBSERVATIONS

The first analysis was made with the assumption that the parking structure walls and slabs were infinitely stiff. In addition, the shear deformation of the service core was neglected. The 100K-FT moment produced the moments shown in Figure 3a (these moments could be obtained from a simple moment distribution analysis). The shear induced in the core by the distribution of the applied moment is shown in Figure 3b and is considerably larger than the corresponding 1K shear that would be present in the core just above the parking level.

A second analysis examined the effect of core shear deformation. The 100K-FT moment was applied to a 30'-0" x 30'-0" core, fixed at the base, with 1'-0" thick walls (a moment of inertia $I = 3.38 \times 10^8 \text{ in}^4$ and a shear area $A_v = 8640 \text{ in}^2$). As in the first run the parking structure walls and slabs were assumed to be rigid. The resulting moments are given in Figure 4a and by comparison with Figure 3 it can be seen that the effect of the shear deformation of the core on the induced moments and shears is very significant if the parking structure walls and slabs are assumed to be rigid.

To observe closer the effect of the shear stiffness on the induced moments two additional runs were made, one where the shear area was reduced by a factor of ten to $A_v = 864 \text{ in}^2$ and the other where the shear area was increased by a factor of 10 to $A_v = 86400 \text{ in}^2$. The plots of the induced moments and shears for this case can be seen in Figures 4c and 4d.

To investigate for the effect of the shear area when the base is assumed pinned runs were made using the same model parameters as used for Figure 4. The results of these runs are shown in Figure 5, and show the shear area to have less effect than when the base is fixed.

To observe the effect of the flexibility of the parking structure walls and floor slab another group of computer runs was made. The structure modelled for these runs had a 30'-0" service core with a moment of inertia $I = 3.38 \times 10^8 \text{ in}^4$, and a shear area which was assumed to be infinite. Because the plan dimensions of the parking structure are independent of the service core dimensions two extreme values of the spring constant were chosen. The two spring constants examined were 3000 K/in and 100,000 K/in. For the type of structure being considered the relative stiffness of the perimeter foundation walls was found to be large, and for this reason varying the bending and shear stiffness of the element modelling the perimeter foundation walls would have little influence on the moments and shears in the service core. For this run and the remainder of the computer runs typical perimeter foundation walls having a length of 100', a height of 9'-0" (floor to floor) and a thickness of 8" were used in the model. The results of these runs are shown in Figure 6.

Inspection of Figure 6 shows that varying the parking slab stiffness radically changes the moments when compared to the infinite floor and wall stiffness results (Figure 1), but within the range of floor stiffness considered here there is not a great variation in the core moments.

Figure 7 shows the results when core shear deformation and parking slab stiffness are both included. Comparison with Figure 6 shows that for the low spring stiffness ($k_s = 3000 \text{ K/in}$) there is very little effect due to shear deformation, as would be expected since the shear forces are very small. For the high spring stiffness ($k_s = 100,000 \text{ K/in}$) the shear deformation has a larger effect, but the major influence on the core moment is the floor stiffness and not the core shear deformation.

Figure 8 depicts the combined results of the 100 K-FT moment and the 1K shear when applied to the structure modelled in Figure 7. Such a combination of shear and moment would represent a building of about 20 storeys in height subject to earthquake forces. It can be seen that the degree of fixity of the core base is the most important parameter in determining the core moments and shears, but the floor stiffness also is important in some cases.

Figures 9 and 10 were developed from structures having a 20' x 20' core and a 40' x 40' core respectively (Figure 1). In combining the effect of the moment and shear the 100 K-FT moment was combined with a 3 K shear for the 20 x 20 core, representing a building of about 6 storeys; and the 100 K-FT moment was combined with a 0.5 K shear for the 40 x 40 core, corresponding to a building of about 35 storeys. Comparing Figures 8, 9 and 10 shows that as the stiffness of the core increases the effect of the other parameters on the distribution of the moment and shear becomes less noticeable.

DETERMINATION OF SPRING CONSTANT TO MODEL THE PARKING SLAB STIFFNESS

The concrete floors of the below grade parking structure transmit the reactive forces acting on the service core to the perimeter foundation walls of the parking structure, Figure 11. A finite element model, (Figure 12) of the parking slab and the corresponding portion of the end walls attributable to the stiffness of each floor A_w (Figure 11), was developed to determine the in plane stiffness of the floor system. The deflection of the load points of the finite element analysis, Δ_{FE} , for various floor and service core dimensions, is given in Table 1. To interpolate the results to other floor plan dimensions and layouts the floor was considered to be a beam of span L and loaded as shown in Figure 13. The deflection for the load points can then be expressed as the sum of the following two equations:

$$\begin{aligned}\Delta_B &= \text{bending deflection} \\ &= \frac{1 \times (L-C)^2 \times (L + 2C)}{48EI} \quad (1)\end{aligned}$$

$$\begin{aligned}\Delta_S &= \text{shear deflection} \\ &= \frac{1 \times (L-C)}{4 AvG} \quad (2)\end{aligned}$$

$$\text{Where } I = \frac{tB^3}{12} + A_w \frac{(B)^2}{2}, \quad Av = tB \quad \text{and} \quad G = \frac{E}{2(1 + \nu)} \approx \frac{E}{2.5}$$

The deflection predicted by the sum of these two equations provides a good estimate of the computer generated deflections if L is greater than B . If L is less than B the predicted deflection is less than the computer generated deflection. For these cases the computer results show point 1 (Figure 12) to have a deflection appreciably larger than the deflection of point 2. This difference is not accounted for by beam theory and so a third term that accounts for some extensional strains in the direction of the load was added to the bending and shear deflection. This term should be large when B is large but should also reflect the overall size of the service core and floor, and so an equation of the form

$$\Delta_C = \frac{1 (B-D)}{8 Et \sqrt{CD}} \cdot P \quad (3)$$

is suggested where β is an unknown factor. With $\beta = 0.25$ the deflections (and resulting stiffnesses) given by the equation $\Delta = \Delta_B + \Delta_S + \Delta_C$ are within 12% of the finite element deflections for a wide range of plan dimensions. The Δ_C term is dominant for those cases where $B = 3L$. The largest stiffness is provided by the long and narrow parking level structure ($L = 100'$, $B = 300'$) and would appear to peak around the 60,000 k/in value (for $E = 3000$ ksi, $t = 8"$). It is clear from the earlier work that such stiffnesses must be considered in the core analysis.

CONCLUSION

In summary, a simple moment distribution method with the assumption of rigid floor slab does not reflect the actual behaviour of the sub-grade structure. It generally signifies drastic moment reduction and high shear in the core, which is not true in most cases. An analysis including shear deformation of the core and assuming rigid floor slab does provide a more realistic result. However, it still does not model the actual behaviour of the system properly, as it neglects the effect of the stiffness of the retaining wall and the in-plane stiffness of the floor diaphragm. A proper analysis involves accurately assessing the stiffness of the slab, as it is the important link between the service core and the comparatively rigid retaining wall. The degree of fixity of the base of the core has the largest influence on the distribution of forces, and so must be carefully considered.

The analysis indicates that the moment in the core below grade may increase or decrease depending on plan dimensions and section properties of the system. It also indicates that moment reversal in the core, with resulting large shear forces, is unlikely to happen for normal building parameters.

RECOMMENDATIONS

The below grade model of the structure must take into account the core base fixity, the stiffness of the parking level floors, shear deformation of the core, and the flexibility of the side walls of the parking structure.

ACKNOWLEDGEMENTS

The authors are indebted to Mr. Yu Song-Qiao, U.B.C. Visiting Chinese Scholar, for the finite element analysis.

TABLE 1 - FLOOR STIFFNESS COMPARISON

C ft	D ft	A _w in ²	L ft	B ft	Δ _B	Δ _S in x 10 ⁻³	Δ _C	Δ	Δ _{FE}	ERROR %	STIFFNESS k/in
25	25	0	300	100	.27572	.07161	.00391	.35124	.36530	-4	2740
			300	300	.01021	.02387	.01432	.04841	.04904	-1	20390
			100	100	.00679	.01953	.00391	.03223	.03523	-8	28380
			100	300	.00033	.00651	.01432	.02116	.02002	6	49950
			150	100	.03255	.03255	.00391	.06901	.07504	-8	13330
		1000	300	100	.16967	.07161	.00391	.24519	.25195	-3	3970
			300	300	.00845	.02387	.01432	.04665	.04632	1	21590
			100	100	.00541	.01953	.00391	.02885	.03035	-5	32950
			100	300	.00027	.00651	.01432	.02110	.01999	6	50020
			150	100	.02003	.03255	.00391	.05649	.05938	-5	16840
40	20	1000	300	100	.16467	.06771	.00368	.23606	.24071	-2	4150
			300	300	.00820	.02257	.01289	.04366	.04475	-2	22350
			100	100	.00415	.01563	.00368	.02346	.02652	-12	37710
			100	300	.0021	.00521	.01289	.01831	.01737	5	57570
20	40	1000	300	100	.17087	.07292	.00276	.24655	.25148	-2	3980
			300	300	.00051	.02431	.01197	.04479	.04570	-2	21880
			100	100	.00574	.02083	.00276	.02934	.03123	-6	32020
			100	300	.00029	.00694	.01197	.01920	.01785	8	56020

E = 3000 ksi ν = 0.25 t = 8"

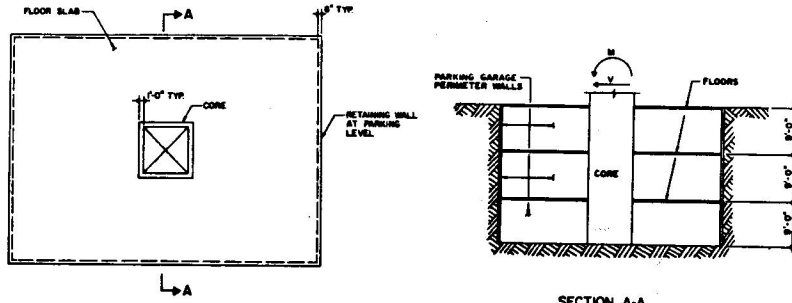


FIG. 1 TYPICAL FLOOR PLAN

SECTION A-A

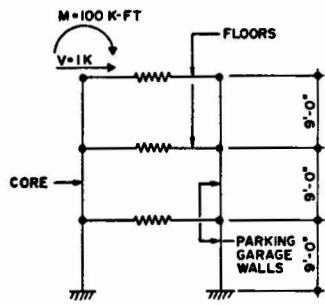


FIG. 2 COMPUTER MODEL

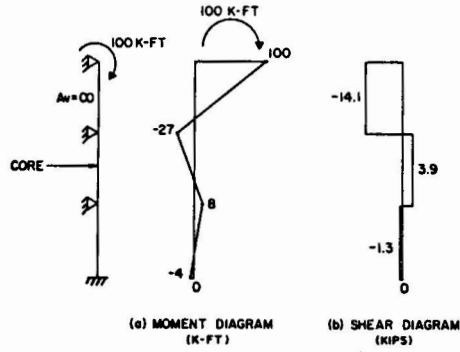


FIG. 3 MOMENT AND SHEAR DIAGRAMS WITH RIGID SUPPORTS

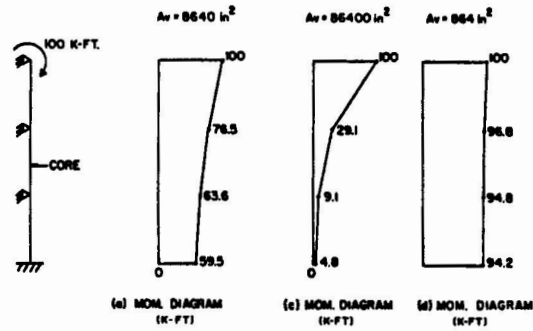


FIG. 4 CORE MOMENT DIAGRAMS FOR VARIOUS SHEAR AREAS

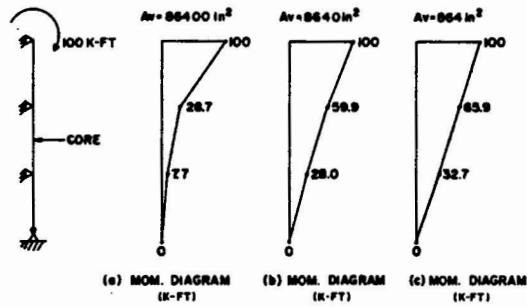


FIG. 5 CORE MOMENT DIAGRAMS FOR VARIOUS SHEAR AREAS

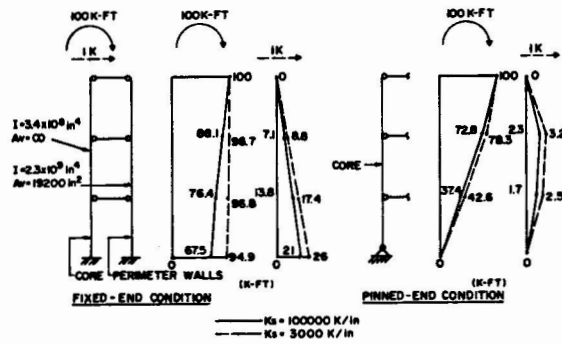


FIG. 6 CORE MOMENT DIAGRAMS FOR DIFFERENT FLOOR STIFFNESSES

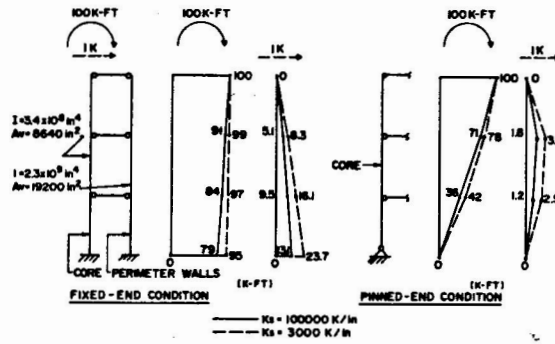


FIG. 7 CORE MOMENT DIAGRAMS FOR DIFFERENT FLOOR STIFFNESSES

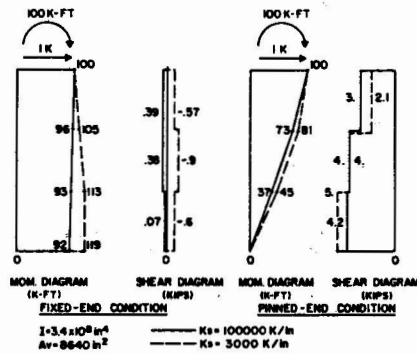


FIG. 8 MOMENT AND SHEAR DIAGRAMS FOR A 30' x 30' CORE

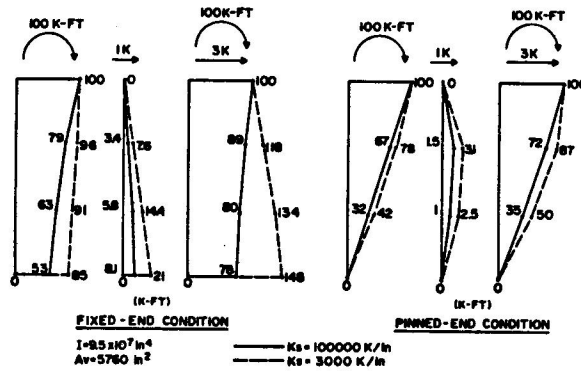


FIG. 9 MOMENT DIAGRAMS FOR A 20' x 20' CORE

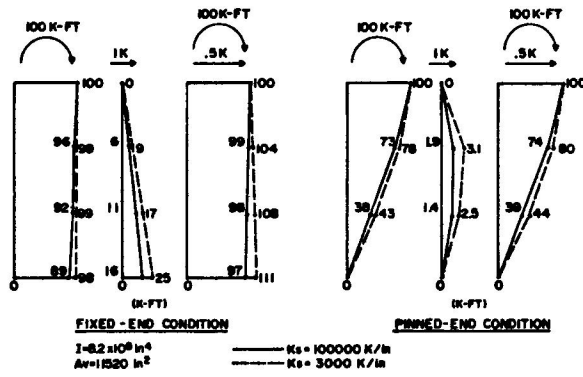


FIG. 10 MOMENT DIAGRAMS FOR A 40' x 40' CORE

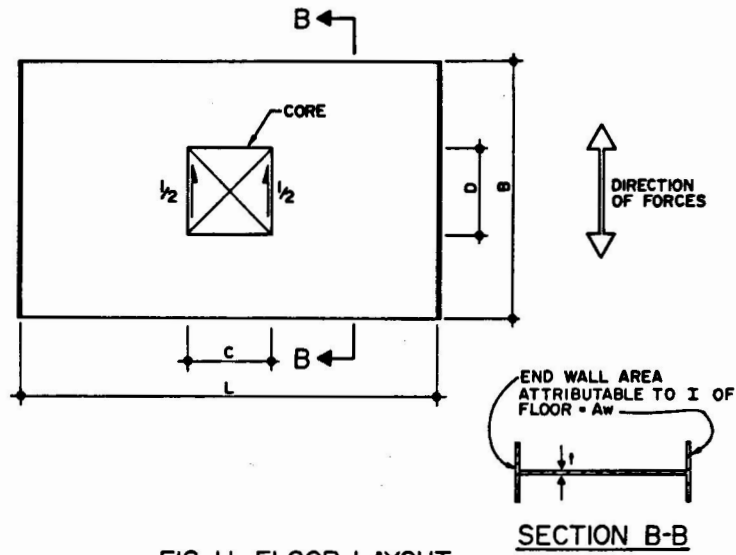


FIG. 11 FLOOR LAYOUT

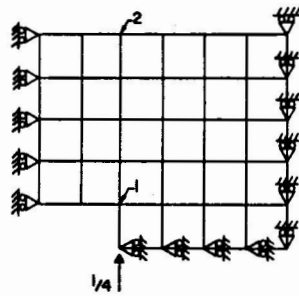


FIG. 12 TYPICAL FINITE ELEMENT MESH USING DOUBLE SYMMETRY

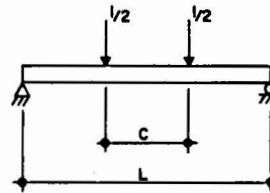


FIG. 13 EQUIVALENT BEAM